JOURNAL OF AIRCRAFT
Vol. 41, No. 2, March–April 2004

Swashplateless Helicopter Rotor with Trailing-Edge Flaps

Jinwei Shen* and Inderjit Chopra†
University of Maryland, College Park, Maryland 20742

A helicopter primary control system with trailing-edge flaps was investigated numerically for its potential to replace a conventional swashplate system. Eliminating the swashplate and associated control system can lead to significant reductions in weight, drag, and cost and an improvement of rotor performance. A comprehensive rotorcraft analysis was developed for analyzing the swashplateless rotor configuration and was implemented to examine the actuation requirements for rotor primary control with trailing-edge flaps. A multicyclic controller was implemented with the swashplateless rotor analysis, and the feasibility of trailing-edge flap performing both primary control and active vibration control was examined. Flap control inputs of a swashplateless rotor are presented at several advance ratios. With optimal selection of blade collective pitch index angle, the flap was shown to be able to trim the rotor with moderate flap inputs. Simulations of flaps performing both primary control and active vibration control were carried out, with the conclusion that trailing-edge flaps are capable of trimming the rotor and minimizing vibratory rotor hub loads simultaneously.

Nomenclature

C_T	=	rotor thrust coefficient
c	=	blade chord
c_d	=	section drag coefficient
c_h	=	section flap-hinge-moment coefficient
c_l	=	section lift coefficient
c_{lf}	=	section flap-hinge-lift coefficient
c_m	=	section pitch-moment coefficient
F_x	=	N_b/rev longitudinal vibratory hub force
F_y	=	N_b/rev lateral vibratory hub force
F_z	=	N_b/rev vertical vibratory hub force
M	=	Mach number
M_x	=	N_b/rev roll vibratory hub moment
M_y	=	N_b/rev pitch vibratory hub moment
N_b	=	number of rotor blades
R	=	rotor radius
W_z	=	weighting matrix for hub loads
$W_{\Delta\theta}$	=	weighting matrix for flap control input rates
W_θ	=	weighting matrix for flap control inputs
z	=	vector of components of hub loads
α	=	angle of attack
δ	=	flap deflection (positive flap down)
δ_0	=	flap collective deflection
δ_{1c}	=	flap lateral cyclic deflection
δ_{1s}	=	flap longitudinal cyclic deflection
θ	=	blade section pitch (positive nose upward)
θ_{index}	=	blade index angle (positive nose upward)
θ_0	=	blade collective pitch
θ_{1c}	=	blade lateral cyclic pitch
θ_{1s}	=	blade longitudinal cyclic pitch
μ	=	advance ratio
σ	=	rotor solidity
ϕ_{twist}	=	elastic torsion deflection (positive nose upward)
ψ	=	azimuth angle

Subscripts

$0, 1c, 1s, \ldots,$ pc, ps, $\ldots, \infty$	=	harmonics of a sine/cosine Fourier-series representation of a periodic function

Presented as Paper 2002-1444 at the 2002 Structural Dynamics and Materials Conference, Denver, CO, 22 April 2002; received 25 June 2002; revision received 9 July 2003; accepted for publication 11 July 2003.

*Graduate Research Assistant, Alfred Gessow Rotorcraft Center, Department of Aerospace Engineering. Student Member AIAA.

†Alfred Gessow Professor and Director, Alfred Gessow Rotorcraft Center, Department of Aerospace Engineering. Fellow AIAA.

Introduction

FLIGHT-CONTROL devices have characteristically been some of the most complex and flight critical components on a helicopter. They generally have numerous exposed linkages, bearings, swashplate, push rods, and hinges. These components are maintenance intensive, costly, and act as a significant source of drag. The basic swashplate control concept was invented in the 1930s and is overall a successful design. However, the weight, drag, and cost, as well as the probability of failure of the mechanical components of swashplate control system, provide an impetus to search for alternative forms of main rotor pitch control.

A wide range of potentially suitable concepts was studied by various researchers. The concepts can be classified into categories according to their method of operation as displayed here:

1) *Blade camber control* is achieved by cyclic excitation with embedded material that is arranged differently on the top and bottom surfaces of the blade sections. Because of the lack of availability of suitable smart materials with sufficient stroke and stiffness, this concept was found to be infeasible.[1]

2) *Blade twist control* enables blade twist to be generated from embedded active materials and via the application of a cyclic differential voltage over the span of the blade. Problems with this design include blade structural integrity and requirement for large actuation power.[2]

3) *Blade pitch control* actuates individual blades in pitch using hydraulic or smart material actuators in the rotating frame. Hydraulic actuation requires implementation of complex hydraulic slipring, whereas smart actuation is limited by the relatively small stroke of current smart materials.[3]

4) *Tilting shaft concept* affects a tilt of the control mast in order to reorient the direction of the rotor thrust. This concept was found to be infeasible because of the unacceptably large actuation forces and strokes required and because of the inherent complexity and weight of the actuation mechanism. This concept is most seen on autogyro.[4]

5) *Active servo flaps* are auxiliary airfoil sections that are located aft of the trailing edge of the main blades as adopted by Kaman. This design involves exposed linkages resulting in large drag penalties.[5,6]

6) *Active plain trailing-edge flaps* are flaps integrated with the main lifting section of the blade are deflected cyclically in order to change the lift and/or moment characteristics of the blade section.[7]

With the recent emergence of smart material actuators of high energy density, it appears promising to apply this technology to primary rotor controls through the application of active trailing-edge

Table 1 MDART rotor and flap properties

Properties	Design value
MDART rotor data	
Rotor type	Bearingless
Number of blades	5
Rotor diameter	34 ft
Rotor speed	392 rpm
Chord	$0.0492R$
Linear twist angle	-10 deg
Solidity	0.078
Trailing-edge flap data	
Flap type	Plain flap
Spanwise length	36 in. (0.18R)
Chordwise size	35% (blade chord)
Flap midspan location	0.83R
Flap hinge overhang	10% (airfoil chord)

flaps.[8] This will involve the integration of smart sensors and actuators, on-blade aerodynamic control surfaces, and integral blade twist. Trailing-edge flap rotors have also received considerable interests among rotorcraft engineers to reduce helicopter vibration and noise.[9–14] The use of a trailing-edge flap rotor for primary control appears attractive in the context of an actively controlled rotor, where embedded flaps can perform multiple functions. The active plain trailing-edge flap can be further classified into lift flap and moment flap based on the dominant load mechanism. It was found that lift flaps require large flap deflections that are infeasible with current smart material technology, whereas moment flaps require comparatively small flap deflections, especially with incorporation of blade pitch indexing.

Recently, Ormiston[7] carried out a very fundamental study on this topic using a simple rigid-rotor model. Lemnios and Jones[5] and Wei and Jones[6] presented modeling and correlation for Kaman's SH-2 rotor that uses a servo-flap-type system for primary control. Straub and Charles[15] examined the preliminary requirement of the swashplateless design for an advanced rotor and control system concept. Virtually all of the recent studies[9–14] of rotor with trailing-edge flaps focused on hub vibration minimization or rotor noise reduction for the conventional rotor with swashplate primary control system. The objectives of this study are as follows:

1) Develop a comprehensive rotorcraft analysis that includes a swashplateless rotor with trailing-edge flaps, and investigate the feasibility of a trailing-edge flap primary control system.

2) Implement multicyclic controller with swashplateless rotor analysis, and examine the capability of trailing-edge flap performing both primary control and active vibration control functions.

3) Explore the actuation requirements under different flight conditions.

The baseline rotor used in the present study is the McDonnell-Douglas Advanced Rotor Technology (MDART) rotor. The MDART rotor is a modern five-bladed preproduction MD900 bearingless rotor. The rotor characteristics are given in Table 1.

Analytical Model

The baseline rotor analysis is taken from UMARC (University of Maryland Advanced Rotorcraft Code).[16] The present analysis incorporates finite element methodology in space and time. The blade is modeled as an elastic beam undergoing flap bending, lag bending, elastic twist, and axial deformation. The rotor blades are discretized into a finite number of beam elements, each with 15 degrees of freedom. The flexbeam and torque-tube consist of four and three beam elements, respectively. Twelve elements are used for the main blade and one element for the swept tip. The coupled blade response and the trim control settings were solved simultaneously for the wind-tunnel trim condition. Eight time elements with sixth-order shape functions were used to calculate coupled trim solution. The trailing-edge flap motion is prescribed, and the actuator dynamics is neglected for this study.[13] However, flap inertial effects are included both in the formulation of the blade equations of motion and the hub loads computation.

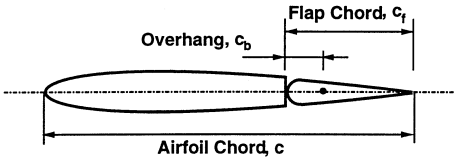

Fig. 1 Trailing-edge flap with aerodynamic balance (nose overhang).

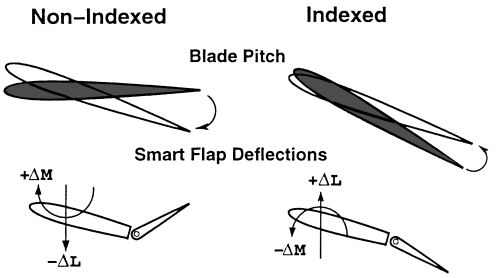

Fig. 2 Blade-pitch indexing.

Aerodynamics of a Flapped Airfoil

A quasi-steady model adapted from Theodorsen's theory[17] is used to model the aerodynamically balanced flap (Fig. 1). Trailing-edge flap aerodynamic balance (nose overhang) was incorporated to vary the aerodynamic characteristics of the airfoil/flap in order to reduce flap hinge moments and, as a result, actuation power.[18] Flap nose overhang is defined as the hinge offset from the leading edge of the flap in terms of the full chord of the airfoil. A typical overhang value places the flap hinge at 10% chord from the leading edge of the flap. For a 35% chord flap this translates into an overhang of approximately 29% of the flap chord. The Theodorsen model considers the flap gap sealed, that is, no leak of fluid between the flap and the base airfoil. A table look-up model based on test data is also used for the correlations. The blade aerodynamic section coefficients (c_l, c_d, c_m) and flap aerodynamic coefficients (c_h, c_{lf}) are looked up in the table for the airfoil angle of attack α, Mach number M, and trailing-edge flap deflection δ.

Analysis of Swashplateless Rotor

For a conventional rotor with a swashplate control system, lifting or lowering of the swashplate disks changes blade collective pitch, whereas forward or side tilting of the swashplate disks governs the cyclic pitch. The trim variables for a conventional helicopter are blade collective pitch θ_0 and cyclic pitch θ_{1c} and θ_{1s}. The present swashplateless rotor design modifies the baseline rotor by replacing the pitch link assembly with a linear root spring. The torque tube is unaltered in the swashplateless rotor design and serves as an aerodynamic fairing, as well as providing in-plane blade damping together with the snubber. For a swashplateless rotor with trailing-edge flap concept, the flaps produce pitching-moment changes, which impel the main blades to pitch against the root spring to achieve aerodynamic equilibrium, thereby producing the desired collective and cyclic blade twist. The trim variables for a swashplateless rotor are flap collective deflection δ_0 and cyclic deflections δ_{1c} and δ_{1s}.

To reduce control actuation forces, the rotor must be designed with torsionally soft blades, which can be achieved using soft root springs at their root. For reducing the flap traveling range, the rotor blades need to be pitched with a nose-up preset angle, which is normally higher than is required to trim the helicopter. As the rotor is accelerated to its rotational speed, the additional nose-down pitching moment generated by the flaps will twist the blade to the desired pitch position. This blade pitch index angle (Fig. 2) is an important design parameter that affects actuation requirements. For a nonindexed blade the flaps need to be deflected up enormously, approximately 20 deg, in order to twist the blade nose up to achieve the desired angles of attack. However, for a pitch indexed blade the flaps are required to have a small downward deflection to obtain a nose-down pitching moment on the blade. This downward deflection of flaps generates additional upward lift on the blade that will

Table 2 Prescribed shaft angles in different forward speeds (positive is tilt forward)

Advance ratio, μ	Shaft angle α_s, deg
0	0
0.05	0.5
0.10	1.1
0.15	2.6
0.20	4.9
0.25	6.9
0.30	8.8
0.35	10.9

move the blade airload distribution inboard and improve the rotor performance in hover and forward flight conditions.[6,7]

For a swashplateless rotor with flaps, the control angle input to the blade is given by

$$\delta(\psi) = \delta_0 + \delta_{1c}\cos(\psi) + \delta_{1s}\sin(\psi) \tag{1}$$

and the blade pitch angle consists of the blade index angle and the elastic twist induced by flap control inputs,

$$\theta(\psi) = \theta_{\text{index}} + \phi_{\text{twist}}(\psi) \tag{2}$$

The flap control angles are obtained from the coupled trim procedure. The coupled analysis determines the blade response for a given set of controls, shaft orientation, and inflow, and provides the blade loads together with the fixed system hub loads. In turn, these loads and responses are used in a separate set of equations representing a prescribed wind-tunnel operating condition. These equations govern the rotor control settings. A typical wind-tunnel experimental procedure involves adjusting the controls to achieve zero first harmonic blade flapping and a prescribed C_T/σ with prescribed shaft angles (Table 2).

Trailing-Edge Flap Performing Multiple Functions

It is attractive to use the trailing-edge flaps for both primary control and active vibration control in order to reduce overall system weight and cost. The trailing-edge flap required to minimize N_b/rev fixed system hub loads are actuated at higher harmonics of rotational speed, typically at (N_b-1, N_b, N_b+1)/rev. For active vibration control the trailing-edge flap input to the blade is

$$\delta(\psi) = \sum_p [\delta_{\text{pc}}\cos(p\psi) + \delta_{\text{ps}}\sin(p\psi)] \tag{3}$$

where $p = N_b - 1, N_b, N_b + 1$. For a five-bladed rotor the trailing-edge flap inputs used in the present study are 4, 5, and 6/rev. A multicyclic controller[19] is used to determine the flap active control inputs (δ_{pc}, δ_{ps}). This algorithm is based on minimization of an objective function,

$$J \equiv \boldsymbol{z}_n^T W_z \boldsymbol{z}_n + \boldsymbol{\theta}_n^T W_\theta \boldsymbol{\theta}_n + \boldsymbol{\Delta\theta}_n^T W_{\Delta\theta} \boldsymbol{\Delta\theta}_n \tag{4}$$

where $\boldsymbol{z}_n$ is a hub loads vector containing the cosine and sine coefficients of the N_b/rev fixed system hub loads F_x, F_y, F_z, M_x, and M_y at time step n. $\boldsymbol{\theta}_n$ and $\boldsymbol{\Delta\theta}_n$ represent the harmonics of the control inputs and control rates, respectively. The diagonal matrices W contain weights for different harmonics of the vibration W_z, the control inputs W_θ, and the control rates $W_{\Delta\theta}$.

Results and Discussion

Before the results of a swashplateless rotor with flaps are investigated, the predictive capability of present comprehensive analysis is evaluated for a baseline bearingless rotor (without trailing-edge flaps) by comparing calculated pitch control settings and blade structural moments with wind-tunnel test data for the MDART rotor. Testing was conducted on the full-scale MDART rotor in the NASA Ames' 40 by 80 foot wind tunnel in 1994 (Ref. 20). The calculated results with active trailing-edge flaps are then compared with CAMRAD II predictions.[14] Following this, the predicted results

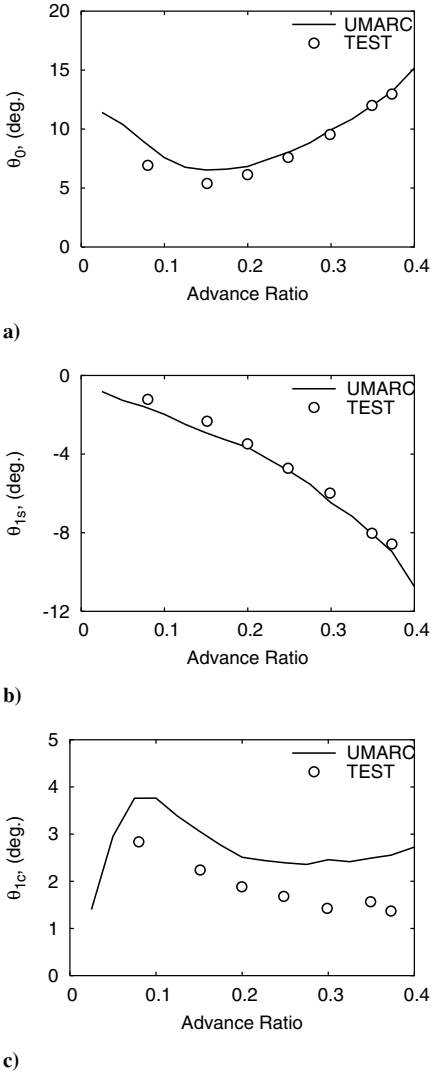

Fig. 3 Measured and predicted control settings θ_0, θ_{1c}, θ_{1s} vs advance ratio μ (conventional swashplate control system): a) collective pitch θ_0, b) longitudinal cyclic θ_{1s}, and c) lateral cyclic θ_{1c}.

of the swashplateless rotor with the embedded flaps are presented, and the effect of blade index angle is then investigated. The active trailing-edge flap rotor and swashplateless rotor have the same blade structural properties and rotor configuration as the MDART rotor (Table 1) with the exception that the swashplateless rotor uses a softer root spring.

Baseline Correlation

Figure 3 shows the predicted and measured values for blade collective pitch, longitudinal pitch, and lateral cyclic pitch for different advance ratios. Figure 3a shows good agreement between predicted and measured collective control angle except a slightly overprediction at low advance ratios. Figure 3b illustrates that the longitudinal control angle agrees well with the test data for the complete range of advance ratios. Figure 3c shows fair agreement on lateral cyclic pitch θ_{1c} at low advance ratio; however, the analysis predicts a somewhat different trend with increasing advance ratio. Lateral cyclic is, in general, sensitive to inflow modeling and blade flapping dynamics.

Figure 4 compares the measured and calculated blade structural moments at an advance ratio of 0.2. The wind-tunnel test data were obtained from measurements over one rotor revolution, filtered to 10 harmonics. Figure 4a shows the blade flapwise bending moments at $r/R = 0.21$. The flapwise bending moments are well captured except the high-frequency content. Figure 4b shows blade chordwise bending moments at $r/R = 0.59$, and good agreement is observed. Figure 4c illustrates blade torsional moments at $r/R = 0.75$.

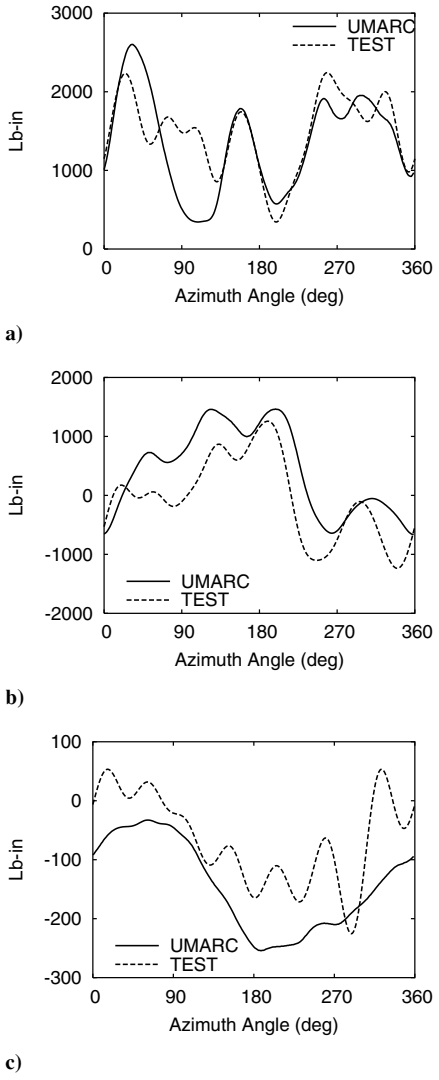

Fig. 4 Measured and predicted blade bending and torsional moment (conventional swashplate control system) for $\mu = 0.2$ and $C_T/\sigma = 0.074$: a) flap bending moment at $r/R = 0.21$, b) chord bending moment at $r/R = 0.59$, and c) torsional moment at $r/R = 0.75$.

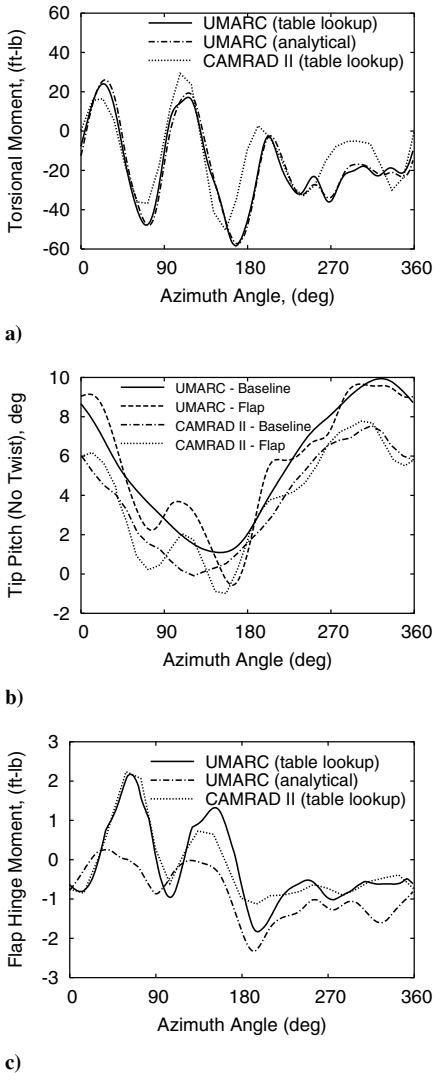

Fig. 5 Predictions of UMARC and CAMRAD II with trailing-edge flap motion $\delta = 2$ deg $\cos(4\psi - 240$ deg) for $\mu = 0.2$ and $C_T/\sigma = 0.075$: a) torsional moment at $r/R = 0.6$, b) blade-tip pitch (excluding built-in twist) with and without trailing-edge flap control, and c) flap hinge moment.

Although the overall trend is captured, the high-frequency components are not predicted well.

Correlation of Trailing-Edge Flap Rotor

Figures 5 compares the predictions of present analysis with CAMRAD II calculations with an active flap input of $\delta = 2$ deg $\cos(4\psi - 240$ deg) at an advance ratio of 0.2. Figure 5a shows the blade torsion moment variation for one complete revolution at 60% radial station. The present predictions show relatively good agreement with CAMRAD II results, with some small differences between predictions obtained by present analysis using table look-up and analytical expressions. Figure 5b illustrates the blade-tip pitch response (control inputs and blade elastic torsion, excluding built-in twist) for the baseline case (zero flap input) and with the flap control activated. The pitch motions for the baseline case agree well except a roughly 2-deg offset between the two analyses. In the active flap case it is observed that approximately the same amount of pitch motion was induced by the trailing-edge flap on the advancing blades. Figure 5c compares flap-hinge-moment predictions from present analysis using table look-up and using analytical expressions with CAMRAD II calculations (using table look-up). Hinge-moment predictions utilizing table look-up agree reasonably well with the CAMRAD II results. Predictions with analytical expressions qualitatively agree with calculations using table look-up; however, there is a considerable quantitative difference, in particular with the magnitude in the first quadrant.

Swashplateless Rotor Predictions

The swashplateless rotor system is a modified version of MDART rotor. A softer root spring is used to replace the pitch link assembly and achieve a rotating fundamental torsional frequency of 2.1/rev in a vacuum condition. For comparison purposes, the conventional rotor used in this section exhibits the same torsional frequency as the swashplateless rotor configuration. This is achieved by adjusting the control system stiffness of the conventional rotor. The trailing-edge flap characteristics are given in Table 1.

Figure 6 compares conventional and swashplateless rotor pitch angles for the complete range of advance ratios ($\mu = 0$ to 0.35). The blade pitch angles are obtained at 75% blade station. The swashplateless rotor has a pitch index angle of 16 deg. The figure shows that the swashplateless rotor is successfully trimmed with the trailing-edge flap control in the complete range of advance ratios. Figure 6a shows collective blade pitch of the swashplateless rotor exhibiting smaller θ_0 than the conventional rotor at advance ratios below 0.30. This is because the collective angle of the flap is downward at advance ratios below 0.30 (Fig. 6d), and this results in favorably additional lift from the trailing-edge flaps, which in turn reduces the required blade pitch angles. At an advance ratio of 0.35, the trailing-edge flap is collectively deflected 4 deg upward, which generates adverse negative lift. This is compensated by a half-degree increase of main blade pitch as shown in Fig. 6a. Figures 6b and 6c compare the blade cyclic pitch of the conventional rotor with the swashplateless configuration. As expected, similar

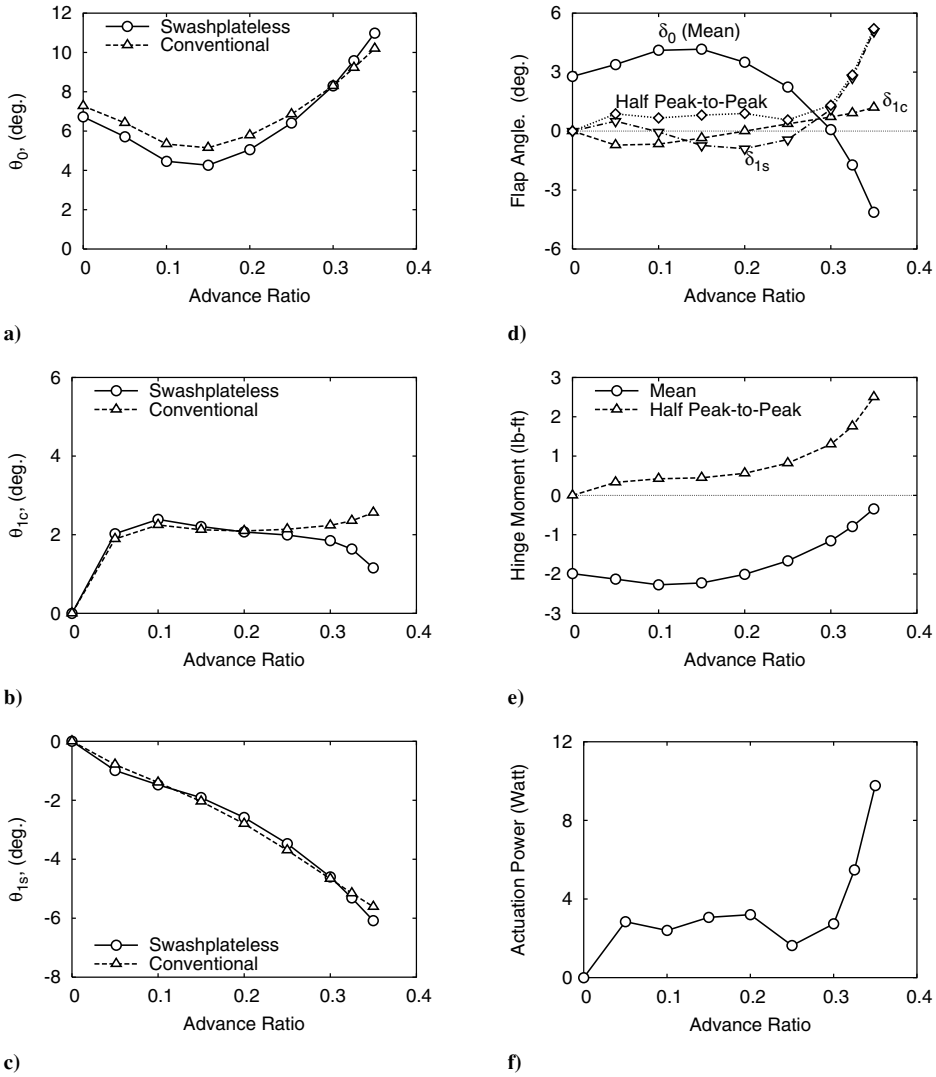

Fig. 6 Comparison of conventional and swashplateless rotor at different forward speeds, blade pitch index angle of 16°, $C_T/\sigma = 0.075$: a) collective pitch at 75%R, θ_0, b) lateral cyclic at 75%R, θ_{1c}, c) longitudinal cyclic at 75%R, θ_{1s}, d) trailing-edge flap deflections, e) trailing-edge flap hinge moment, and f) trailing-edge flap actuation power.

trends are observed between the two rotor configurations. The difference is attributed to the additional lift generated by the flap cyclic deflections.

Figure 6d presents the trailing-edge flap deflection required to trim the swashplateless rotor. The blade index angle of the swashplateless rotor, 16 deg, is larger than the required blade pitch at advance ratios below 0.30. Trailing-edge flap collective angle δ_0 is deflected downward for μ below 0.30 to bring the blade pitch down, while δ_0 is deflected upward at advance ratio of 0.35 to further twist the blade nose up to the desired position. The longitudinal cyclic δ_{1s} presents small variation at advance ratios below 0.25 and increases largely above advance ratio of 0.25. This is because of the cyclic twist effect of rotor blade from the flap collective angle δ_0 under the lateral asymmetric aerodynamic environment in forward flight conditions. A downward-deflected δ_0 twists the blade nose down more in the advancing side of the rotor than the retreating side because of difference of tangential velocities, and this results in a desirable blade longitudinal cyclic twist used to trim the rotor. As shown at advance ratios of 0.1 and 0.25, this blade cyclic twist resulted from trailing-edge flap collective deflection; δ_0 is sufficient to trim the rotor as the required trailing-edge longitudinal cyclic, and δ_{1s} is almost zero. A similar effect is seen for the blade lateral cyclic twist because of the flap collective deflections. However, trailing-edge flap lateral cyclic δ_{1c} is generally small because of the small required values of blade lateral cyclic pitch. Overall, the required half peak-to-peak values of trailing-edge flap deflections are shown below 6 deg, whereas the mean values are below 5 deg in the complete range of advance ratios.

Figure 6e illustrates the mean and half peak-to-peak values of the flap hinge moments at several advance ratios. Because of the use of aerodynamic balance overhang, the hinge moments are relatively small in the complete range of advance ratios. Amplitude of mean hinge moments generally reduces with advance ratio because the flap collective δ_0 is decreasing with respect to advance ratio. Half peak-to peak values of hinge moments increases with respect to advance ratio primarily because of increment of trailing-edge flap travel range and the aggravation of unsteady aerodynamic environment.

Figure 6f presents the actuation power for the swashplateless rotor at several advance ratios. The actuation power is the mean value of the positive product of the hinge moment and flap input rate and is essentially dominated by the flap deflection amplitude and rate. At an advance ratio of 0.25, the actuation power is at minimum because the half peak-to-peak trailing-edge flap deflections are at minimum (Fig. 6d).

Blade-Pitch Indexing

Blade-pitch index angle is a key design parameter, and its effect on the flap actuation requirements is examined in Fig. 7. Figure 7a presents the flap deflections as a function of blade pitch index angles at an advance ratio of 0.2. Both the mean and half peak-to-peak amplitude of the flap deflection are shown decreasing initially with

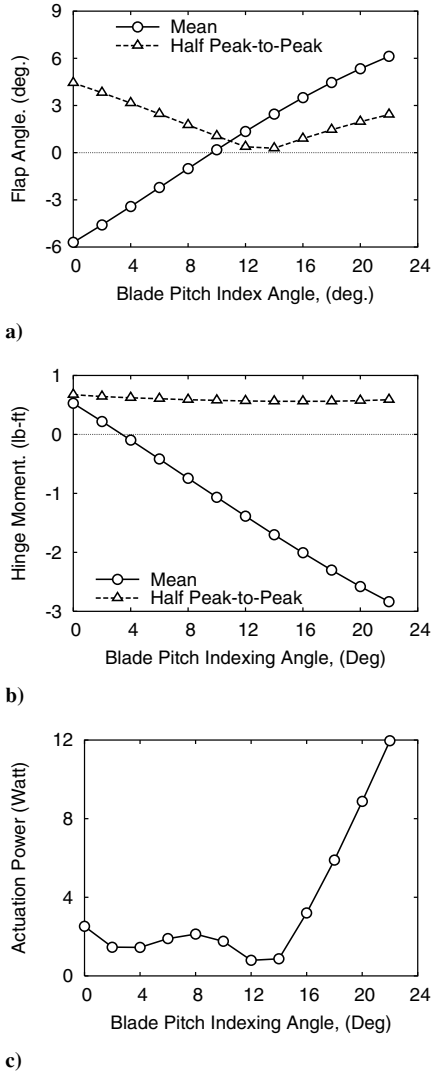

Fig. 7 Effect of blade-pitch index angle on trailing-edge flap deflections and actuation requirement, advance ratio of 0.2 and $C_T/\sigma = 0.075$: a) trailing-edge flap angle, b) flap hinge moment, and c) flap actuation power.

increasing index angle. The mean and half peak-to-peak values reach a minimal value for index angles of 10 and 14 deg, respectively, and increase thereafter with higher index angle. The decreasing of mean values of flap deflection δ_0 is because of the required blade collective pitch that is reduced with higher index angle. The half peak-to-peak values of flap deflection are reduced because of the favorable blade-cyclic-twist effect induced by flap collective deflection δ_0 in the asymmetric aerodynamic environment. Figure 7b illustrates the hinge-moment changes with respect to the blade-pitch index angle. The half peak-to-peak component of the hinge moment shows small variations with the blade index angle. The mean values turns from a nose-up hinge moment at zero index angle to nose-down moment for index angle below 4 deg because the required flap collective deflection gradually changes from upward deflections, −6 deg at zero index angle, to a downward deflection, 6 deg at index angle of 22 deg (Fig. 7a). Figure 7c presents the actuation power, which shows a small variation with index angle before 14 deg and increases largely after that because of the increasing of both mean and half peak-to-peak components of trailing-edge flap deflections as shown in Fig. 7a.

Trailing-Edge Flap Performing Multiple Functions

Predictions with a trailing-edge flap performing both primary control and active vibration control are shown in Figs. 8. Figure 8a illustrates the flap input requirements to provide primary control

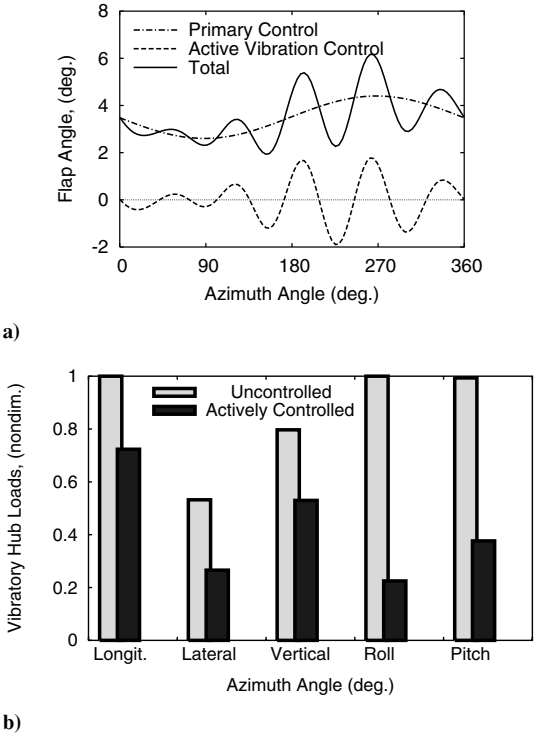

Fig. 8 Trailing-edge flap performing both functions of primary control and active vibration control, advance ratio of 0.2, $C_T/\sigma = 0.075$, and blade-pitch index angle of 16 deg: a) trailing-edge flap input and b) 5/rev vibratory hub loads minimization.

and active vibration control for a complete rotor revolution at an advance ratio of 0.2. The total flap inputs required for both primary control and active control are between 2 to 6 deg. Figure 8b compares the 5/rev vibratory hub loads of the swashplateless rotor with and without active flap inputs for vibration reduction. The weighting parameters on the hub loads are {0.04, 2.3, 1.0, 0.44, 0.136}, acting on hub axial, side force, and normal force, and rolling moment and pitching moment, respectively. Maximum reduction is shown with hub rolling moments, which have a 78% reduction, whereas minimum reductions with hub longitudinal force have a 27% reduction. Overall, the objective function J [Eq. (4)] is reduced by 83%.

Conclusions

A comprehensive rotorcraft analysis for a swashplateless rotor with trailing-edge flaps was developed, and the actuation requirements of a primary control system was evaluated. A multicyclic controller was implemented with the swashplateless rotor analysis, and the feasibility of trailing-edge flap performing both primary control and active vibration control was examined.

Predictions of control settings and blade structural moments were correlated with MDART wind-tunnel test data. Good overall agreement was observed. Calculations of blade torsional moment and blade-tip pitch, as well as trailing-edge flap hinge moments, are compared with predictions from CAMRAD II with an active trailing-edge flap input. Again, it shows reasonably good agreement.

The swashplateless rotor was shown to be trimmed successfully with trailing-edge flap control system in the complete range of advance ratios. With a blade pitch index angle of 16 deg, the required half peak-to-peak values of trailing-edge flap deflections are below 6 deg, whereas the mean values are below 5 deg. Trailing-edge flap hinge moments are small because of the use of aerodynamic balance overhang in the trailing-edge flap design, and this in turn resulted in small actuation power requirements in the complete range of advance ratios.

The blade-pitch index angle was found to be a key design parameter for a feasible swashplateless rotor system. An optimally selected pitch index angle was shown to decrease substantially the actuation

requirement. The advantages of using blade-pitch index are that it 1) reduces the trailing-edge flap collective deflection δ_0 and 2) decreases the trailing-edge flap cyclic deflection δ_{1c} and δ_{1s} through the desirable blade cyclic twist induced by downward deflected δ_0 in the asymmetric rotor aerodynamic condition of a forward-flying helicopter.

Trailing-edge flaps were shown to be able to perform both primary control and active vibration control functions. It was observed that the rotor was trimmed and the objective function consisting of vibratory hub loads was reduced approximately 83% with the trailing-edge flap deflections with a range between 2 to 6 deg at advance ratio of 0.2 and a blade-pitch index angle of 16 deg. The requirements of swashplateless rotor with trailing-edge flaps in maneuvering and autorotation flights are not studied in this paper although they must be met in the swashplateless rotor design.

References

[1]Straub, F. K., "A Feasibility Study of Using Smart Materials for Rotorcraft," *Smart Materials and Structures*, Vol. 5, No. 1, 1995, pp. 1–10.

[2]Bueter, A., Ehlert, U.-C., Sachau, D., and Breitbach, E., "Adaptive Rotor Blade Concepts: Direct Twist and Camber Variation," *Active Control Technology for Enhanced Performance Operational Capabilities of Military Aircraft, Land Vehicles and Sea Vehicles*, AIAA, Reston, VA, June 2001, p. 11.

[3]Ham, N. D., "Helicopter Individual-Blade-Control and Its Applications," *American Helicopter Society 39th Annual Forum Proceedings*, American Helicopter Society, Alexandria, VA, 1983, pp. 613–623.

[4]Houston, S. S., "Identification of Autogyro Longitudinal Stability and Control Characteristics," *Journal of Guidance, Control, and Dynamics*, Vol. 21, No. 3, 1998, pp. 391–399.

[5]Lemnios, A. Z., and Jones, R., "The Servo Flap—An Advanced Rotor Control System," *Proceedings of AHS and NASA Ames Research Center Vertical Lift Aircraft Design Conference*, American Helicopter Society, Alexandria, VA, 1990, pp. 1–41.

[6]Wei, F.-S., and Jones, R., "Correlation and Analysis for SH-2F 101 Rotor," *Journal of Aircraft*, Vol. 25, No. 7, 1988, pp. 647–652.

[7]Ormiston, R. A., "Aeroelastic Considerations for Rotorcraft Primary Control with on-Blade Elevons," *American Helicopter Society 57th Annual Forum Proceedings*, American Helicopter Society, Alexandria, VA, 2001, pp. 1–17.

[8]Chopra, I., "Status of Application of Smart Structures Technology to Rotorcraft Systems," *Journal of the American Helicopter Society*, Vol. 45, No. 4, 2000, pp. 228–252.

[9]Millott, T., and Friedmann, P., "Vibration Reduction in Helicopter Rotors Using an Actively Controlled Partial Span Trailing Edge Flap Located on the Blades," NASA Tech. Rept. CR 4611, June 1994.

[10]Milgram, J., and Chopra, I., "A Parametric Design Study for Actively Controlled Trailing Edge Flaps," *Journal of the American Helicopter Society*, Vol. 43, No. 2, 1998, pp. 110–119.

[11]Milgram, J., Chopra, I., and Straub, F., "Rotors with Trailing Edge Flaps: Analysis and Comparison with Experimental Data," *Journal of the American Helicopter Society*, Vol. 43, No. 4, 1998, pp. 319–332.

[12]Shen, J., and Chopra, I., "Aeroelastic Modeling of Trailing-Edge Flaps with Smart Material Actuators," *Proceedings of the 41st AIAA/ASME/ASCE/AHS/ASC Structure, Structural Dynamics, and Materials Conference*, AIAA, Reston, VA, 2000, p. 14.

[13]Shen, J., and Chopra, I., "Aeroelastic Stability of Smart Trailing-Edge Flap Helicopter Rotors," *Proceedings of the 42nd AIAA/ASME/ASCE/AHS/ASC Structure, Structural Dynamics, and Materials Conference*, AIAA, Reston, VA, 2001, p. 11.

[14]Straub, F. K., and Charles, B. D., "Aeroelastic Analysis of Rotors with Trailing Edge Flaps Using Comprehensive Codes," *Journal of the American Helicopter Society*, Vol. 46, No. 3, 2001, pp. 192–199.

[15]Straub, F., and Charles, B., "Preliminary Assessment of Advanced Rotor/Control System Concepts (ARCS)," USA AVSCOM, Tech. Rept. 90-D03, U.S. Army Aviation Systems Command, Fort Eustis, VA, Aug. 1990.

[16]Bir, G., and Chopra, I., "University of Maryland Advanced Rotor Code (UMARC) Theory Manual," Center for Rotorcraft Education and Research, Univ. of Maryland, Tech. Rept. UM-AERO 94-18, College Park, July 1994.

[17]Theodorsen, T., and Garrick, I. E., "Nonstationary Flow about a Wing-Aileron-Tab Combination Including Aerodynamic Balance," Tech. Rep. No. 736, NACA, 1942.

[18]Hassan, A. A., Straub, F. K., and Noonan, K. W., "Experimental/Numerical Evaluation of Integral Trailing Edge Flaps for Helicopter Rotor Applications," *Proceedings of the American Helicopter Society 56th Annual Forum*, Virginia Beach, VA, May 2-4 2000, pp. 84–102.

[19]Johnson, W., "Self-Tuning Regulators for Multicyclic Control of Helicopter Vibration," NASA Tech. Rept. TP 1996, March 1982.

[20]Nguyen, K., Lauzon, D., and Anand, V., "Computation of Loads on the McDonnell Douglas Advanced Bearingless Rotor," *American Helicopter Society 50th Annual Forum Proceedings*, American Helicopter Society, Alexandria, VA, 1994, pp. 337–346.